Electron temperature fluctuation measurements in the pedestal of improved confinement regimes at ASDEX Upgrade

R. Bielajew[1], G.D. Conway[2], L. Gil[3], A.E. Hubbard[1], P.A. Molina Cabrera[1], D. Silvagni[2,4], E. Viezzer[5], A.E. White[1], and the ASDEX Upgrade Team[2]

[1]*Plasma Science and Fusion Center, MIT, Cambridge, MA, USA*
[2]*Max-Planck-Institut für Plasmaphysik, Boltzmannstr. 2, 85748, Garching, Germany*
[3]*Instituto de Plasmas e Fusão Nuclear, Instituto Superior Técnico, Universidade Lisboa, PT*
[4]*Physik-Dept. E28, Technische Universität München, 85748, Garching, Germany*
[5]*Dept. of Atomic, Molecular and Nuclear Physics, University of Seville, Seville, Spain*

Introduction

Electron temperature fluctuation, δT_e, measurements provide important information on plasma confinement scaling and transitions between L-mode, H-mode, and other improved confinement regimes, as well as the role of "edge modes" in the perpetuation of these regimes. Using Correlation Electron Cyclotron Emission (CECE) at ASDEX Upgrade (AUG), these measurements are obtained with high (4 MHz) temporal and good (4 mm) spatial resolution to study δT_e behavior in three ELM (Edge Localized Mode) free confinement regimes, including:

- Stationary ELM-free H-mode, which has similarities to Enhanced D-alpha (EDA) H-mode at Alcator C-Mod and is attained in AUG by high ECRH heating [1]. The EDA H-mode has an edge-localized quasi-coherent mode (QCM), thought to be responsible for a continuous relaxation of edge pressure gradients [2].
- Quiescent H-mode (QH-mode), which is currently being developed at AUG with low density, unfavorable ∇B direction, and co-NBI. A steady state QH mode has not yet been achieved with tungsten walls. QH mode is accompanied by an Edge Harmonic Oscillation (EHO), which expels impurities in place of ELMs [3, 4].
- I-mode, which has high energy confinement with low particle confinement [5]. A Weakly Coherent Mode (WCM) is often present in the pedestal, and may play a role in the separation of energy and particle (T_e and n_e) confinement channels [6].

These three regimes all allow for high energy confinement while being ELM-free, unlike the standard H-mode.

CECE Diagnostic

A multi-channel CECE radial comb radiometer has been installed and operated at AUG as part of a collaboration with MIT [7, 8]. This diagnostic was recently expanded to include access to a

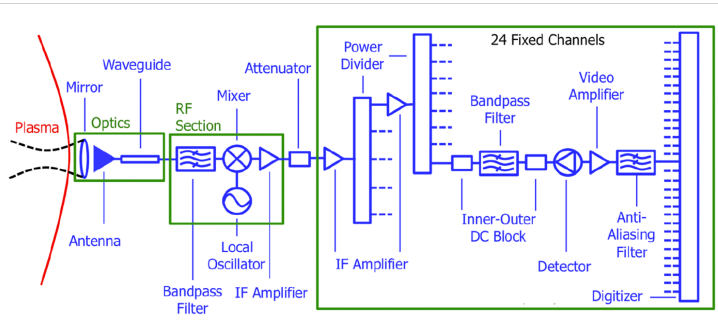

Fig. 1 *Schematic block diagram CECE system at AUG (adapted from [7])*

different vessel port and toroidal location with more favorable optics. The CECE system, shown as a block diagram in Fig. 1, involves waveguide optics, an RF section, an IF section, and a data acquisition system. The optics at the new location include three lenses that result in a 3 cm diameter spot size. The RF down converter section employs a 115 GHz local oscillator which may be adjusted ±2 GHz, plus an upper (117–125 GHz) or lower (105–113 GHz) sideband filter. The RF section antenna may be moved radially by 6.1 cm to optimize the focal point for the desired radial measurement location. The IF section consists of 24 fixed frequency 200 MHz bandwidth filters, with center frequencies from 4 to 8.75 GHz. At a standard AUG B_T field of 2.45 T and standard plasma shape, the channel locations cover a radial range of $\rho_{pol} = 0.9$ out into the scrape-off layer. The exact measurement locations depend on plasma shape and field. Temperature fluctuation measurements in the edge are challenging due to the need for plasma stationarity and sufficient optical thickness($\tau < 2$) [9].

Results

The CECE system has been used to confirm the existence of edge modes and their radial structure in the three improved confinement regimes. For the discharges presently studied, $\tau > 2$ for $\rho_{pol} < 0.99$ during all improved confinement regimes. However, only the stationary ELM-free H-mode discharge had an optically thick L-mode phase. Fig. 2 shows coherence $|\gamma_c(f)|$ spectra of CECE radial channel pairs during L-mode and stationary ELM-free H-mode in the same discharge. The spectra show a coherent mode in the ELM-free H-mode phase at around 30 kHz (lower frequency than the QCM at C-Mod), which is also seen in density (reflectometer) and magnetics (Mirnov coil) signals. Fig. 3 displays radial temperature fluctuation level, $\delta T_e/T_e$, and kinetic profiles of the ELM-free H-mode discharge. The fluctuation level is calculated as $\frac{\delta T_e}{T_e} = \sqrt{\frac{2}{B_{IF}} \int_{f_1}^{f_2} \frac{Re\{\gamma_c - \gamma_{bg}\}}{1 - Re\{\gamma_c - \gamma_{bg}\}}}$ where γ_c and γ_{bg} are the complex and background coherence, B_{IF} is the IF filter bandwidth, and f_1–f_2 is the frequency range of the broadband

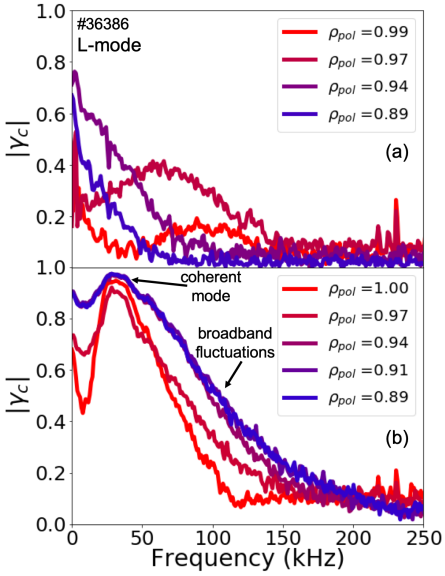

Fig. 2 *Coherence spectra in (a) L-mode and (b) stationary ELM-free H-mode.*

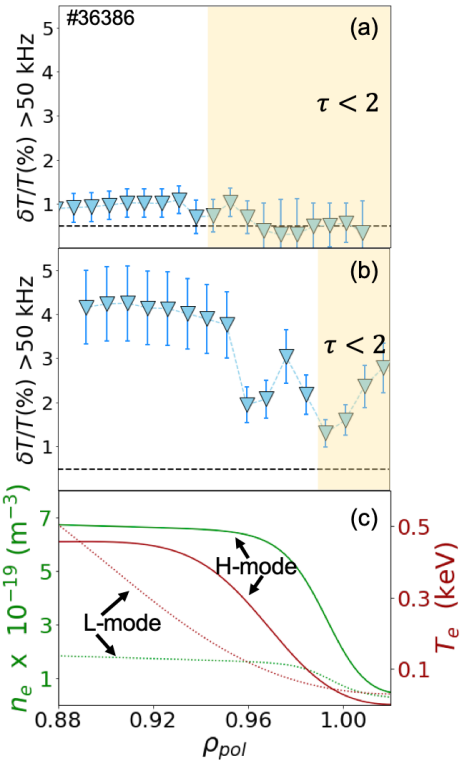

Fig. 3 *Radial properties include broadband $\delta T_e/T_e$ in (a) L-mode and (b) stationary ELM-free H-mode, and (c) the kinetic profiles in L-mode (dashed lines) and stationary ELM-free H-mode (solid lines). The black dashed line in (a) and (b) is the CECE sensitivity limit.*

feature [7]. The L-mode phase is optically thin at $\rho_{pol} > 0.94$, but the temperature fluctuation level in the optically thick region is lower in L-mode than in ELM-free H-mode. In the H-mode phase, the broadband fluctuation level is maximum near $\rho_{pol} = 0.91$ and decreases towards the separatrix. The amplitude of the coherent mode at 30 kHz is also largest at the innermost CECE measurement location, and thus could be interacting with broadband turbulence resulting in the increased $\delta T_e/T_e$ in ELM-free H-mode. The density and temperature pedestals are located at $\rho_{pol} > 0.95$ in the ELM-free H-mode period, so the maximum coherent mode amplitude and broadband fluctuation level occur well inside of the pedestal. The radial width and location of the coherent mode suggest that this could be a different mode than the QCM.

Fig. 4 shows coherence spectra and the radial profile of the broadband $\delta T_e/T_e$ level of a QH-mode "development" discharge. During the transient QH period, the spectra display the EHO fundamental at around 10 kHz as well as a broadband mode centered around 80 kHz. The EHO and its harmonics are also present in density and magnetics spectra. The EHO only appears in CECE channels in the edge and pedestal region and has a maximum amplitude at $\rho_{pol} = 0.98$. The broadband mode appears during the same time period as the EHO and is also localized near the pedestal bottom with $\delta T_e/T_e = 4.3\%$.

Coherence spectra and the $\delta T_e/T_e$ profile of an I-mode discharge are shown in Fig. 5. The WCM appears in the I-mode phase as a 25-125 kHz broadband feature at $\rho_{pol} = 0.98$ with $\delta T_e/T_e = 4.5\%$, while the preceding L-mode phase has no distinct localized mode. This WCM $\delta T_e/T_e$ level is in the range of previous AUG measurements [10].

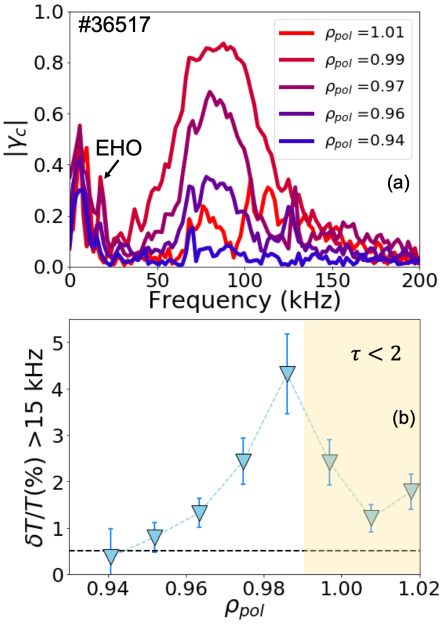

Fig. 4 *Transient QH-mode (a) coherence spectra and (b) the $\delta T_e/T_e$ radial profile*

Discussion

A coherent mode has been identified in stationary ELM-free H-modes, and the EHO has been identified in transient QH-modes. These MHD modes occupy part of the same frequency regime as the broadband fluctuations, but they are coherent enough to be clearly separate features. Care must be taken to separate out these modes from the broadband signals. In I-mode the WCM does not appear as a coherent mode separate from broadband fluctuations, but rather contributes to the broadband spectrum.

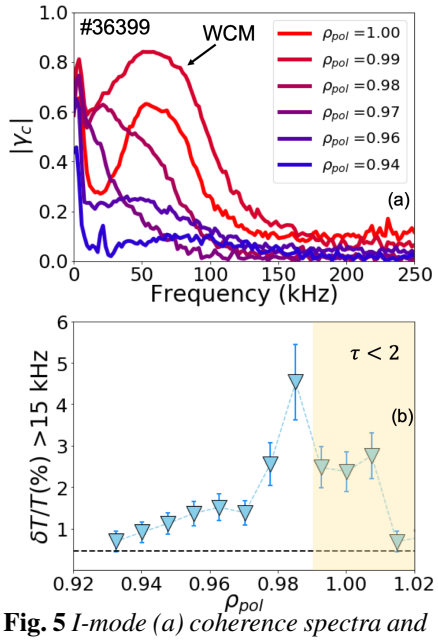

Fig. 5 *I-mode (a) coherence spectra and (b) the $\delta T_e/T_e$ radial profile.*

The finely spaced channels of the CECE comb permit mode localization if the modes are located in the measurement range. The EHO and WCM have been localized to the plasma edge, but the coherent mode in stationary ELM-free H-mode has not yet been fully localized as the radial extent of the CECE channels does not currently extend far enough. Further study of the structure of this mode will assist in the comparison between the EDA H-mode and stationary ELM-free H-modes. Further studies of the differences in broadband turbulence and edge modes between these three regimes, as well as mode and broadband turbulence interactions are ongoing. Quantifying the influence of density fluctuations in low optical depth measurements is also an area of current work and will be important for comparisons between L-mode and improved confinement regimes.

References

[1] L. Gil *Proc. 46th EPS Conf. Plasma Phys. (Milan) 2019 O2.110.*

[2] M. Greenwald *et. al, Plasma Phys. Control. Fusion* **42** A263 (2000).

[3] K.H. Burrell *et. al, Phys. Plasmas* **12** 056121 (2005).

[4] W. Suttrop *et. al, Plasma Phys. Control. Fusion* **46** A151–A156 (2004).

[5] D.G. Whyte *et. al, Nucl. Fusion* **50** 105005 (2010).

[6] P. Manz *et. al, Nucl. Fusion* **55** 083004 (2015).

[7] A.J. Creely *et. al, Rev. Sci. Instrum.* **89** 053503 (2018).

[8] S.J. Freethy *et. al, Phys. Plasmas* **DPP59** 055903 (2018).

[9] M. Bornatici *et. al, Nucl. Fusion* **23** 1153 (1983).

[10] T. Happel *et. al, Plasma Phys. Contol. Fusion* **59** 014004 (2018).

Acknowledgements

This work is supported by the EUROfusion Consortium (No. 633053), the US DoE under Grants DE-SC0006419, DE-SC0014264, and DE- SC0017381, and by NSF GRFP (No. 1122374).